

INTRODUCTION

- Conventional MRI has **limited biological specificity** to the subvoxel composition of tissues
- Relaxation spectroscopic (RS) MRI** methods map **distributions of relaxation parameters** like T1, T2, and mean diffusivities (MD), in microscopic water pools *in vivo*¹⁻³
- Correlation-spectroscopic (CS) MRI** methods further improve specificity⁴⁻⁶ by assessing how **relaxation parameters co-vary** in tissue microenvironments
- We design and evaluate a pulse sequence **with integrated inversion recovery (IR)² and isotropic diffusion encoding (IDE)³** preparations and derive maps of **subvoxel T1-MD spectra** in healthy volunteers

METHODS

- The sequence in **Fig. 1** allows the efficient interleaved multislice acquisition⁷ IR-IDE images with a **wide range of joint T1 and MD weightings**, by independently controlling the (TI,TR) and b-value parameters, respectively
- Assuming slow exchange between microscopic water pools and an adiabatic inversion efficiency¹, η , we can **derive the correlation spectrum** of subvoxel $R_1 = 1/T_1$ and MD properties, $p(R_1, MD)$, from the net signal attenuation in a repeated IR experiment:

$$S_\eta(b, TI, TR) = \int_0^\infty \int_0^\infty \left(1 - 2\frac{\eta}{100} e^{-TI \cdot R_1} + e^{-TR \cdot R_1}\right) e^{-b \cdot \bar{D}} p(R_1, \bar{D}) dR_1 d\bar{D}$$
- We conducted **Monte Carlo simulations**, and CS-MRI experiments in a **polymer diffusion phantom⁸** and **three healthy volunteers** using 16 diffusion weightings ($b=0.05$ - $3.6\text{ms}/\mu\text{m}^2$) and 19 T1-weightings (TI=50-5000ms, including no-IR), TE=98ms, FOV=22cm, 2.5mm in-plane resolution, 5mm slice thickness

Acknowledgements: This work was supported by the NIH BRAIN Initiative grants R24-MH-109068-01 and U01-EB-026996, the Intramural Research Program (IRP) of the NICHD within the NIH, and the CNRM under the auspices of the HJF, grants #309698-4.01-65310, #308049-8.01-60855, CNRM-89-9921. The opinions expressed herein are those of the authors and not necessarily representative of those of the Uniformed Services University of the Health Sciences (USUHS), the Department of Defense (DoD), VA, NIH or any other US government agency, or the Henry M. Jackson Foundation

RESULTS

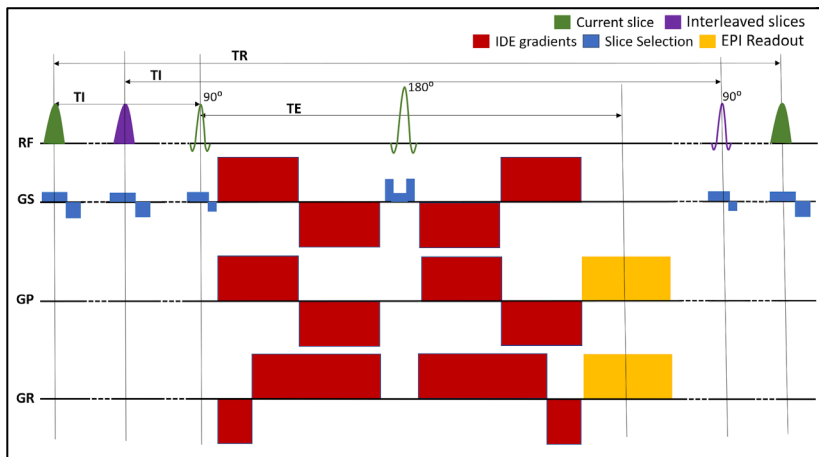


Figure 1: Pulse sequence diagram for multi-slice imaging with integrated IR and IDE preparations. Slice-selective IR and EPI acquisitions are interleaved to maintain the same T1-weighting (TI, TR) for each slice. Multiple scans are acquired with different TI/TR, and multiple b-values in each scan.

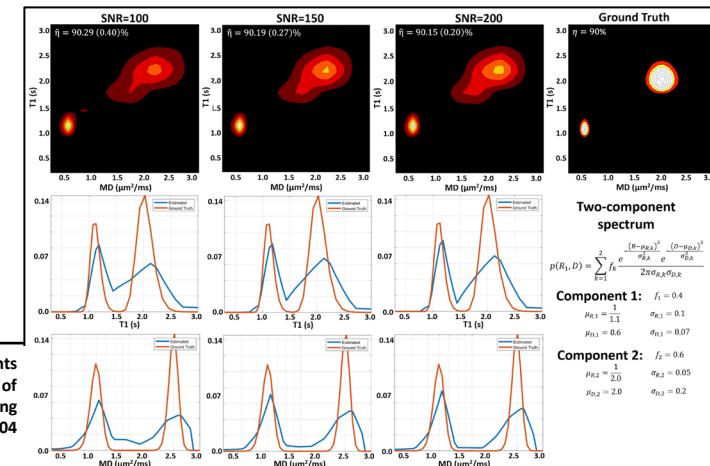


Figure 2: Monte-Carlo experiments illustrating the SNR dependence of reconstructing T1-MD spectra using our experimental protocol with 304 IR-IDE MRIs

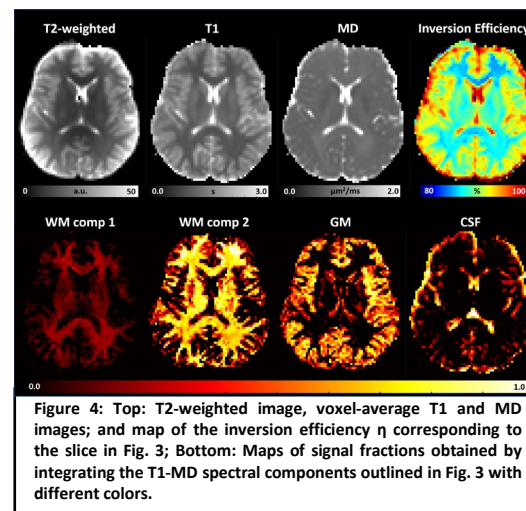
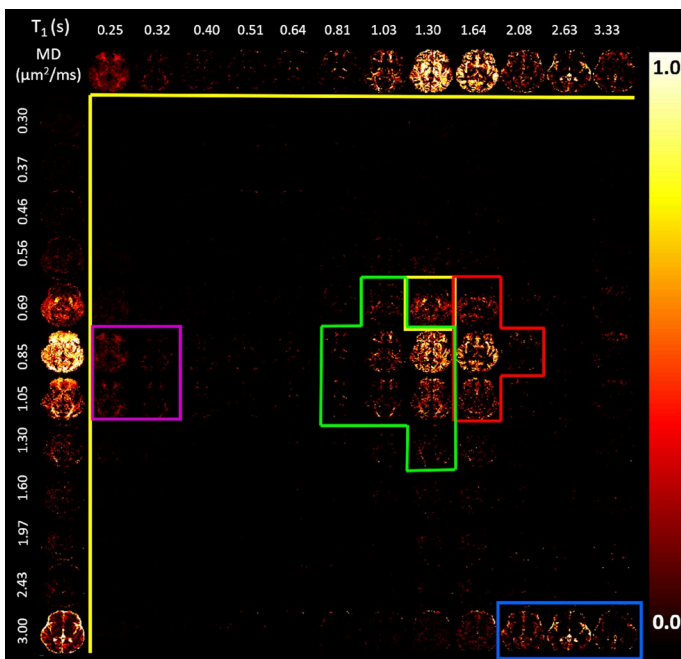


Figure 4: Top: T2-weighted image, voxel-average T1 and MD images; and map of the inversion efficiency η corresponding to the slice in Fig. 3; Bottom: Maps of signal fractions obtained by integrating the T1-MD spectral components outlined in Fig. 3 with different colors.

Figure 3: Maps of 2D normalized T1-MD correlation spectra along with corresponding marginal distributions of subvoxel T1 values (top row) and subvoxel MD values (bottom row) in a healthy volunteer.

DISCUSSION

- Due to the **long TE** needed to accommodate the diffusion gradients, the estimated **T1-MD spectra (Fig. 3) are likely T2-weighted (Fig. 4)**
- Marginal distributions derived from T1-MD spectra (**Fig. 3**) are consistent with previous 1D RS-MRI studies in healthy volunteers^{1,3}
- The two WM components (**Figs. 3, 4**) may reflect effects from **magnetization transfer⁸** and chemical exchange
- The general signal representation in T1-MD CS-MRI may be able to characterize **healthy and diseased tissues** with arbitrary subvoxel heterogeneities
- Mapping the subvoxel landscape of joint T1-MD properties may **improve biological specificity** in the early detection of neurodegenerative diseases, neuroinflammation, cancer, brain injury, and ischemic stroke

References: 1. Labadie et al., MRM, **71**:375 (2014); 2. Mackay et al., MRM, **31**:673 (1994); 3. Avram et al. NIMG **185**:255 (2019); 4. Does et al. MRM **47**:274 (2002); 5. Benjamini et al., NIMG **163**:183 (2017); 6. Kim et al., MRM **78**:2236 (2017); 7. Park et al., MRM **2**:534 (2085); 7. Pierpaoli et al. ISMRM **17**, 1414 (2009); 8. Avram et al., NIMG **53**:132 (2010);